Supplementary Information (SI) for Journal of Materials Chemistry A.
This journal is © The Royal Society of Chemistry 2026

SUPPLEMENTARY INFORMATION

Chemically Recyclable and Room-Temperature Self-Healable Siloxane-Imine Benzoxazine Vitrimers for Soft Magnetic Actuation

Prashansa Gupta,[a] Bhavika Bhatia,[a] Jan-Marten Sprenger,[b,c] Adrian Wolf,[b] Katharina Koschek,[b,d] * Bimlesh Lochab[a*]

[a]Materials Chemistry Laboratory, Department of Chemistry, School of Natural Sciences, Shiv Nadar University, Delhi NCR, Uttar Pradesh 201314, India.

[b]Fraunhofer Institute for Manufacturing Technology and Advanced Materials (IFAM), Wiener Straße 12, 28359 Bremen, Germany

[c]Department of Production Engineering, University of Bremen, Badgasteiner Str. 1, 28359 Bremen, Germany

[d]MAPEX Center for Materials and Processes, 28359 Bremen, Germany

E-mail: bimlesh.lochab@snu.edu.in, katharina.koschek@ifam.fraunhofer.de

Table of Contents

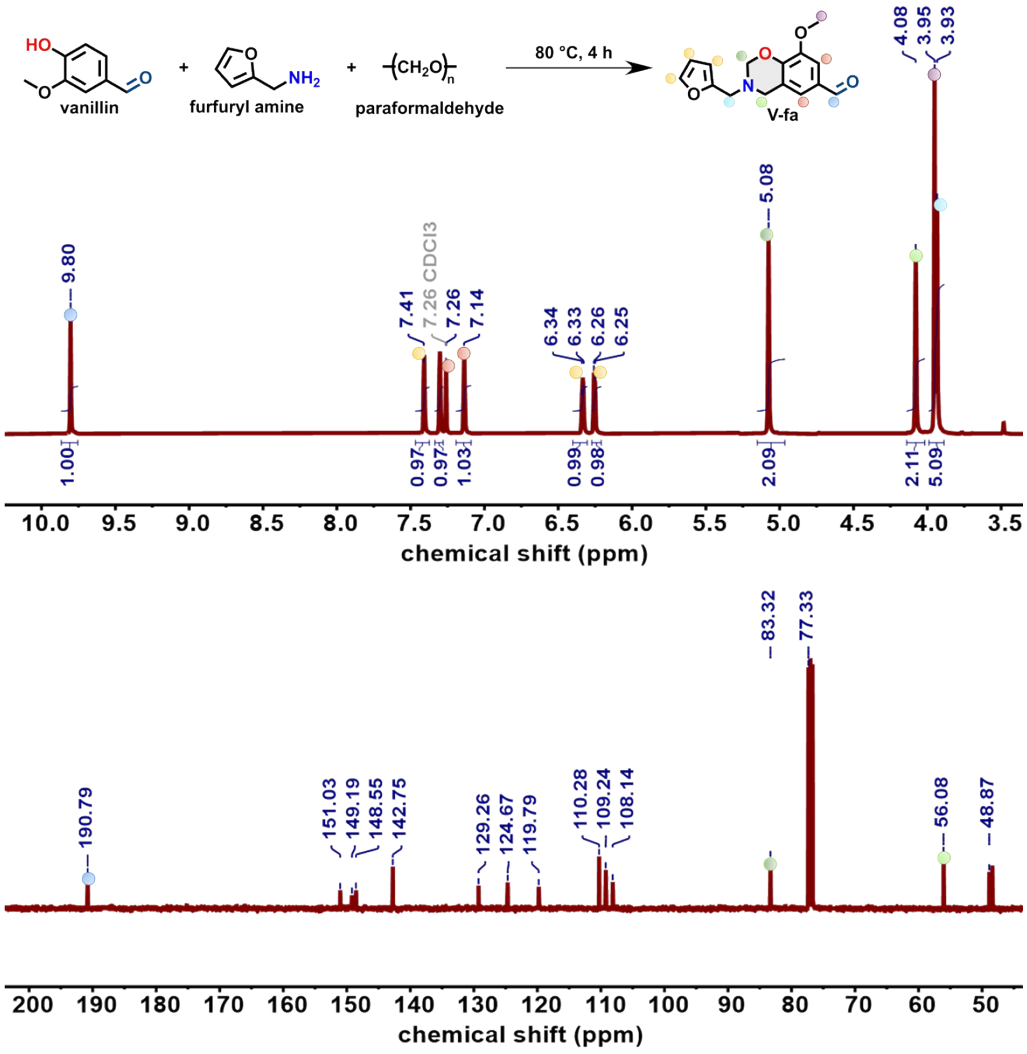

Figure S1. (a) ^{1}H and (b) ^{13}C NMR spectra of Vfa. *Recorded in $CDCl_3$.

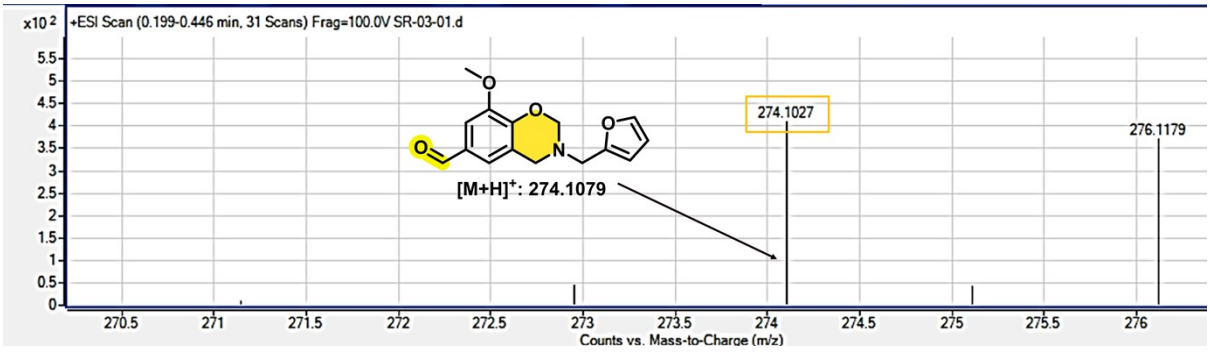

Figure S2. Mass chromatograph of benzoxazine monomer (Vfa).

Table S1. Feed-in ratio of siloxane amine and benzoxazine monomer.

Vfa : Si_{P0}	
w/w%	**Eqv. ratio**
1:10	1: 7.0
1:15	1: 4.6
1:20	1: 3.4
1:25	1: 2.4
1:30	1: 1.6

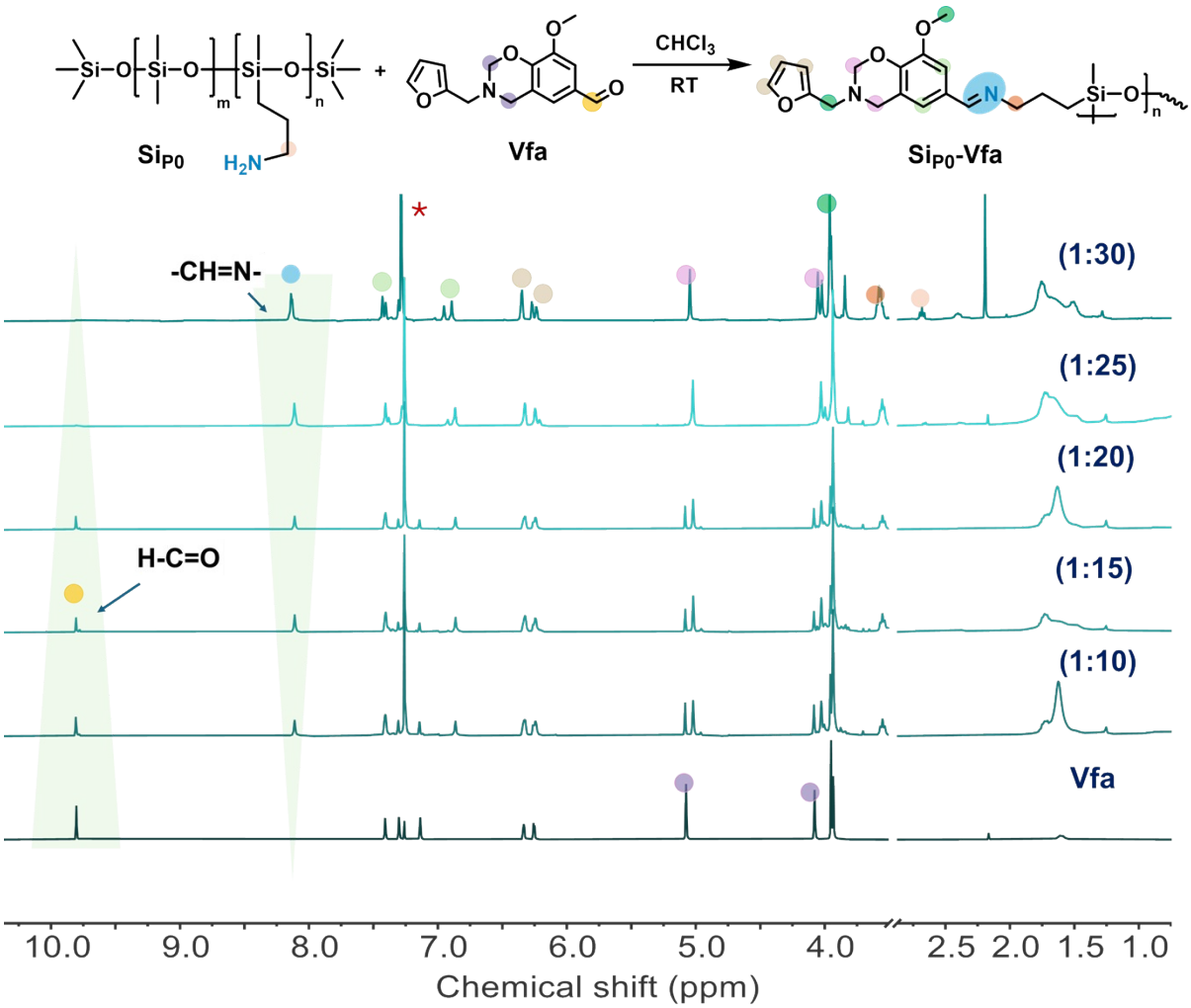

Figure S3. Stacked ^{1}H NMR spectra of Si_{P0}-Vfa for imine bond formation with different stoichiometric ratios of aldehyde (Vfa) to amine (Si_{P0}). *Recorded in $CDCl_3$.

Theoretical calculations of stoichiometric ratio of amine and aldehyde:

$$Amine\ Eq.\ Wt. = \frac{MW\ of amine}{No.\ of\ active\ hydrogens\ in\ amine}$$

$$4400 = \frac{20939\ g.mol^{-1}}{No.\ of\ active\ hydrogens\ in\ amine}$$

$$No\ of\ active\ hydrogens\ in\ amine = 4.8$$

Thus, 1 eq. of amine requires 2.5 eq. of aldehyde.

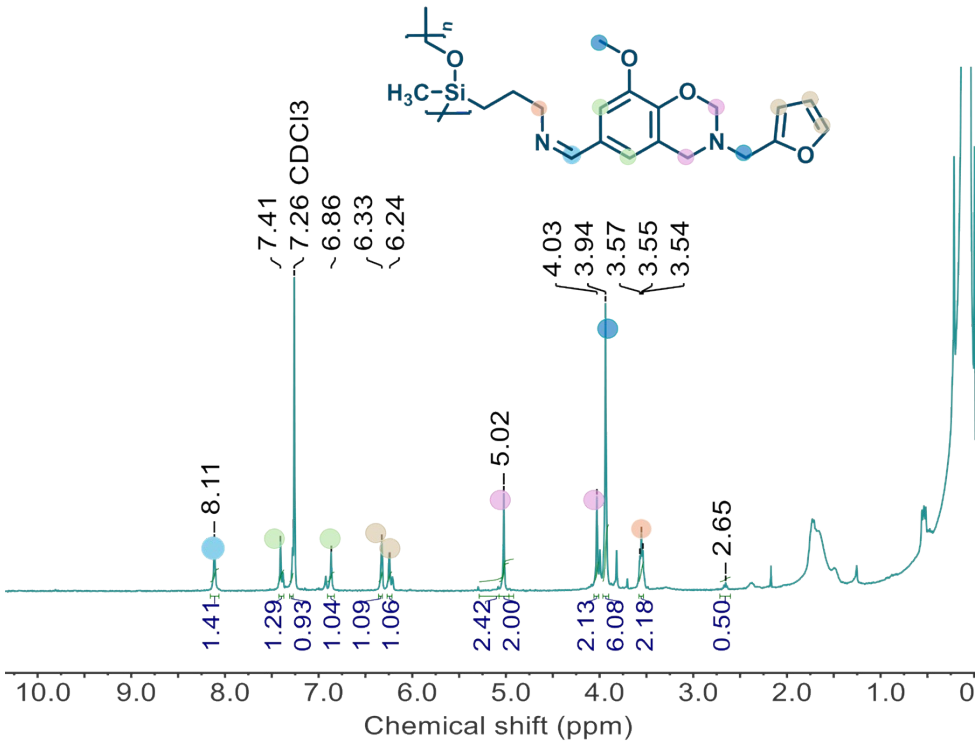

Figure S4. ^{1}H NMR spectra of imine prepolymer (Si_{P0}-Vfa).

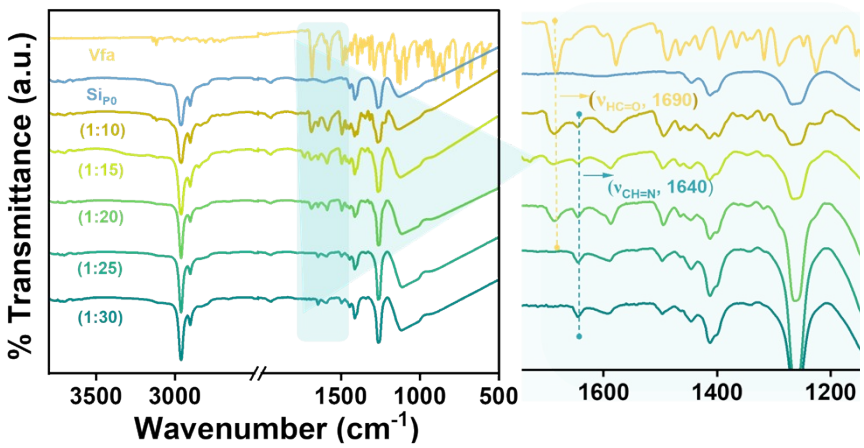

Figure S5. FTIR spectra for Si_{P0}-Vfa prepared with varying stoichiometry.

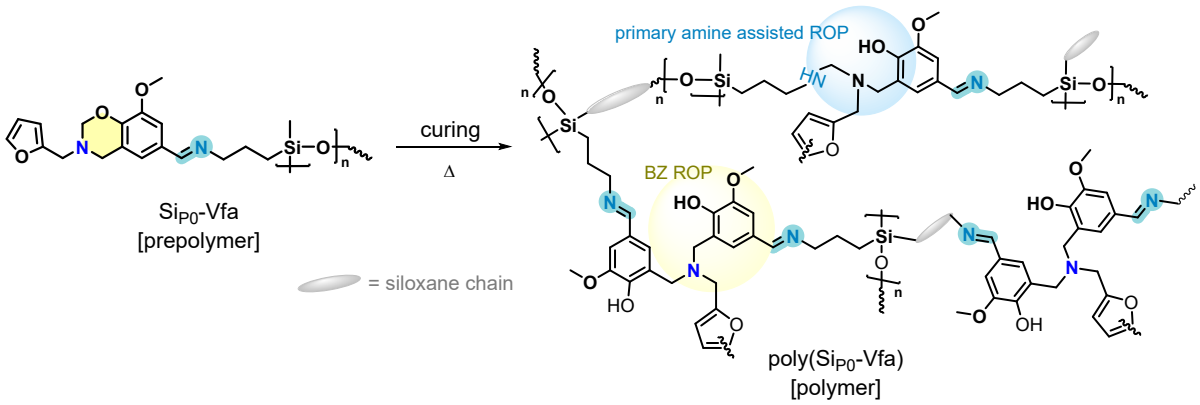

Figure S6. Proposed structure of the polymer network post curing.

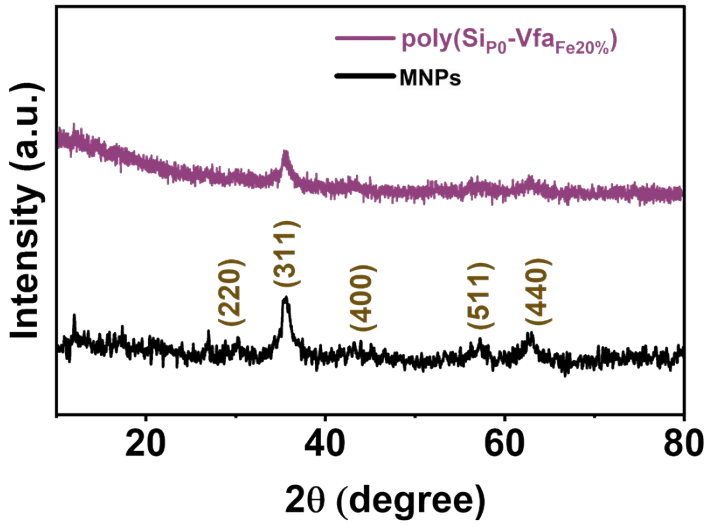

Figure S7. XRD patterns of MNPs and the poly(Si$_{P0}$-Vfa$_{Fe20\%}$) film.

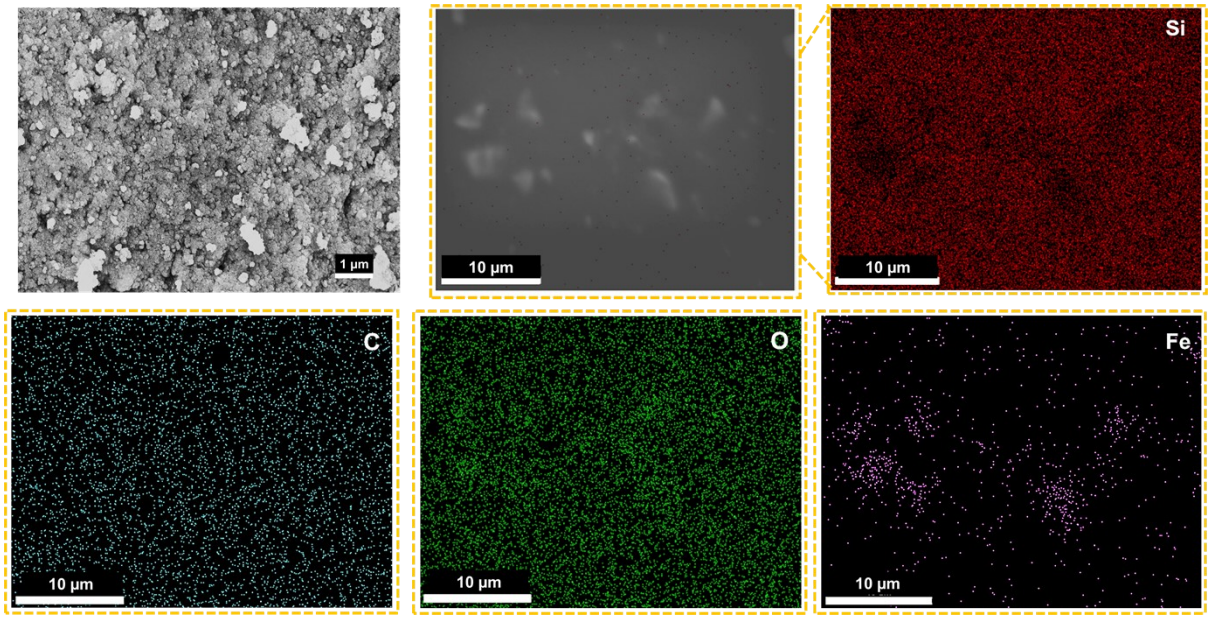

Figure S8. Morphology characterization. SEM images of (a) Fe_3O_4 nanoparticles, (b) poly(Si_{P0}-$Vfa_{Fe20\%}$) polymer film with elemental mapping of poly(Si_{P0}-$Vfa_{Fe20\%}$) polymer film.

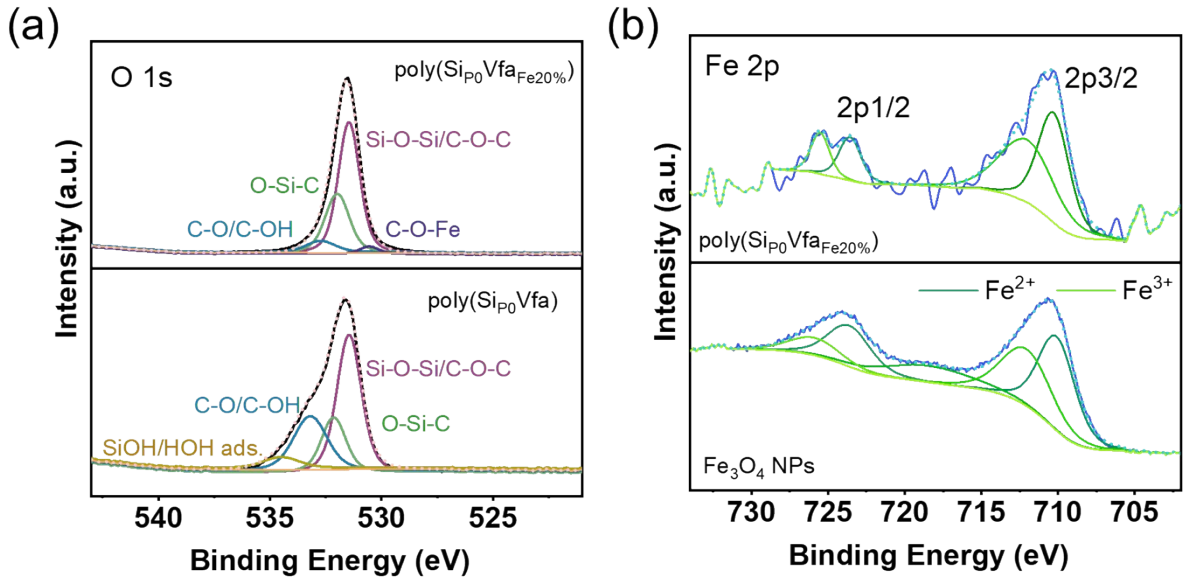

Figure S9. Deconvoluted high-resolution XPS spectra of (a) O 1s for the pristine film and poly(Si_{P0}-$Vfa_{Fe20\%}$) (upper panel), and (b) Fe 2p for Fe_3O_4 nanoparticles (lower panel) and poly(Si_{P0}-$Vfa_{Fe20\%}$) film.

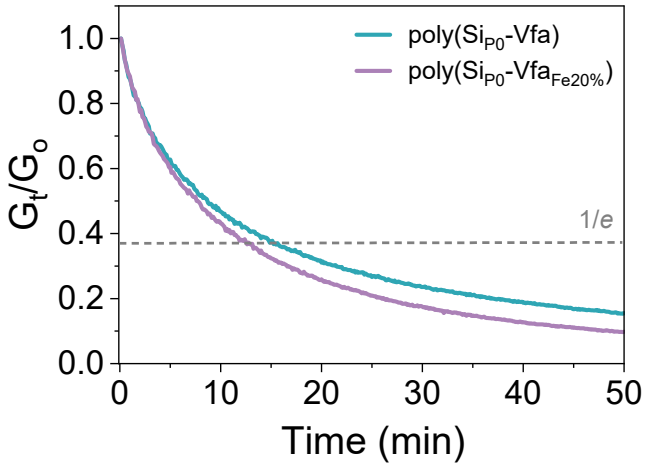

Figure S10. Normalized isothermal stress-relaxation plots at 25 °C at 0.1% strain to show differences in the characteristic relaxation time relaxation curves of both the vitrimers.

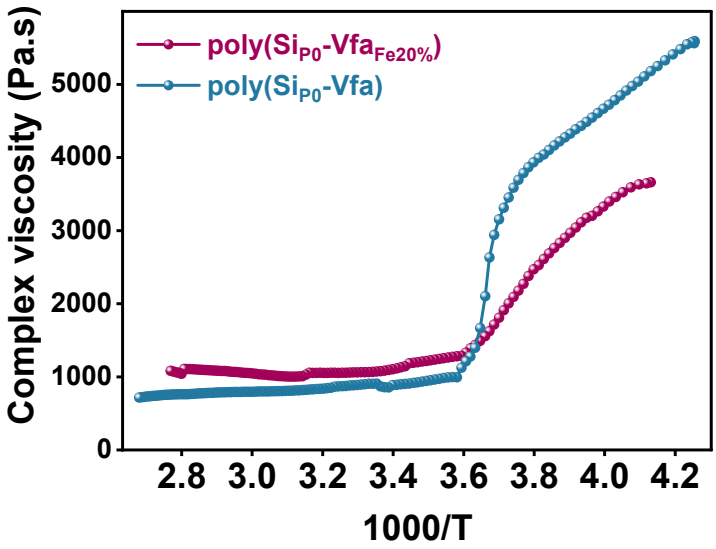

Figure S11. Complex viscosity graph of both the vitrimers w.r.t. temperature.

Calculation of activation energy (E_a)

Arrhenius equation: $\ln(\tau) = Ea/RT + \ln(\tau o)$

Linearity equation from the plot, y = mx + c

(i) For poly(Si$_{P0}$-Vfa):

$\ln(\tau) = 2.57 \times 1000/T - 5.227$

$E_a/R = 2.57 \times 1000$

$E_a = 21.4$ kJ/mol

(ii) For poly(Si_{P0}-$Vfa_{Fe20\%}$):

$\ln(\tau) = 1.37 \times 1000/T + 0.08$

$E_a/R = 1.37 \times 1000$

$E_a = 11.4$ kJ/mol

Calculation of Topology freezing temperature (T_v)

(i) For poly(Si_{P0}-Vfa):

T_v is calculated by extrapolating the viscosity to $\eta = 10^{12}$ Pa.s in the Arrhenius plot of ln η vs $1000/T$

Whereupon, extrapolating to ln (10^{12}) gave us $1000/T_v = 4.83$

$T_v = 1000/4.83 = 207.1$ K = – 66 °C

(ii) For poly(Si_{P0}-$Vfa_{Fe20\%}$):

extrapolating to ln (10^{12}) gave us $1000/T_v = 8.6$

$T_v = 1000/8.6 = 116.3$ K = –156 °C

Figure S12. Magnetic field analysis of the used magnet via Gaussmeter.

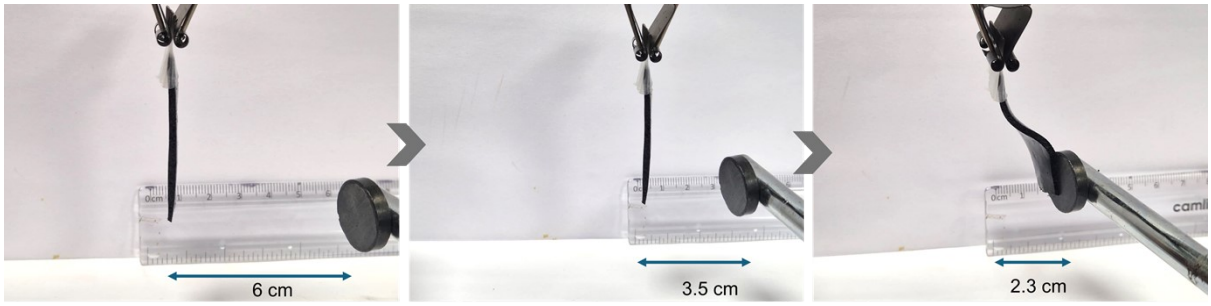

Figure S13. Stroke length analysis of poly(Si_{P0}-$Vfa_{Fe20\%}$) under an external magnetic field of 75 mT, illustrating the bending displacement and actuation response of the magnetic vitrimer.

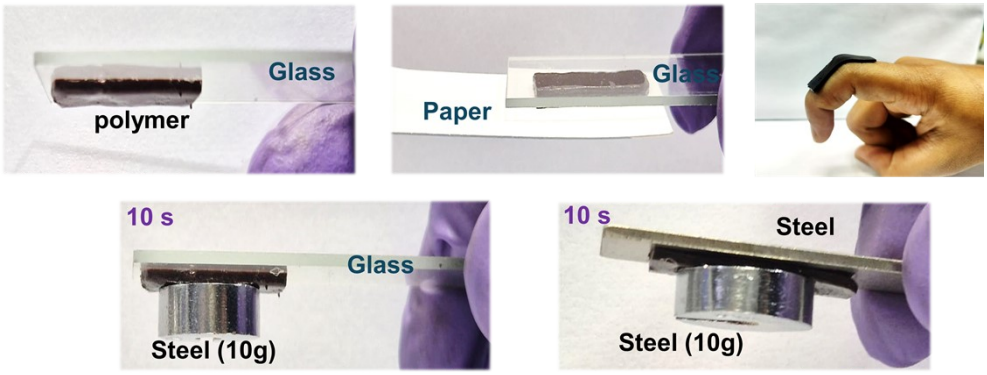

Figure S14. Digital images of surface adhesion of poly(Si_{P0}-Vfa) on different mono-/sandwich substrate.

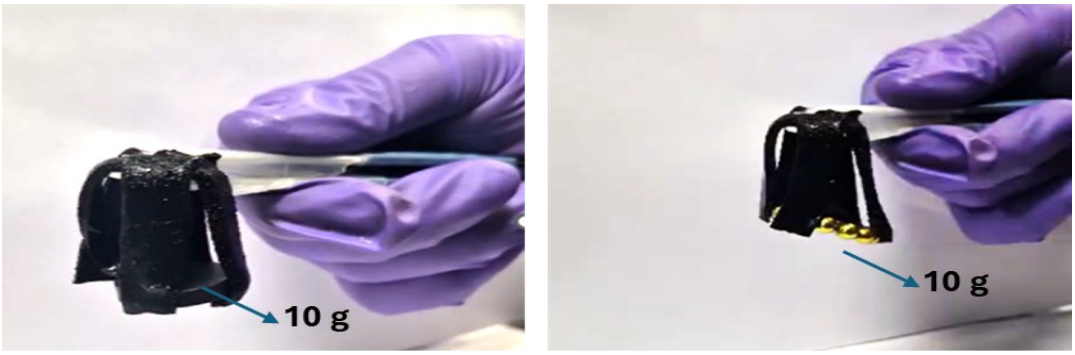

Figure S15. Load-bearing performance of the magnetic vitrimer actuator demonstrating the ability to lift up to 10 g under an external magnetic field of $\leq$ 75 mT, confirming its potential for soft actuation and mild load-responsive applications.

Movie S1. Bending & returning of magnetic responsive film (mp4)

Movie S2. Circular movement of magnetic responsive film (mp4)

Movie S3. Pendulum behaviour (mp4)

Movie S4. Magnetic actuation as gripper (mp4)

Movie S5. Self-healing of vitrimer film (mp4)

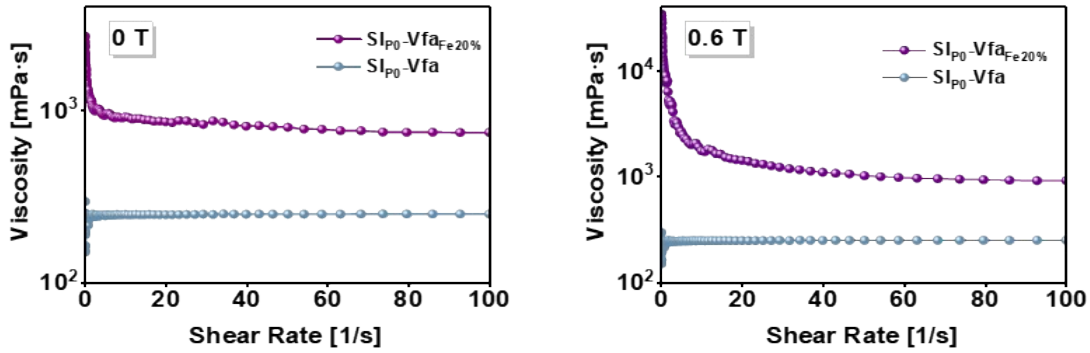

Figure S16. Effect of shear rate on viscosity in prepolymers as a function of magnetic field.

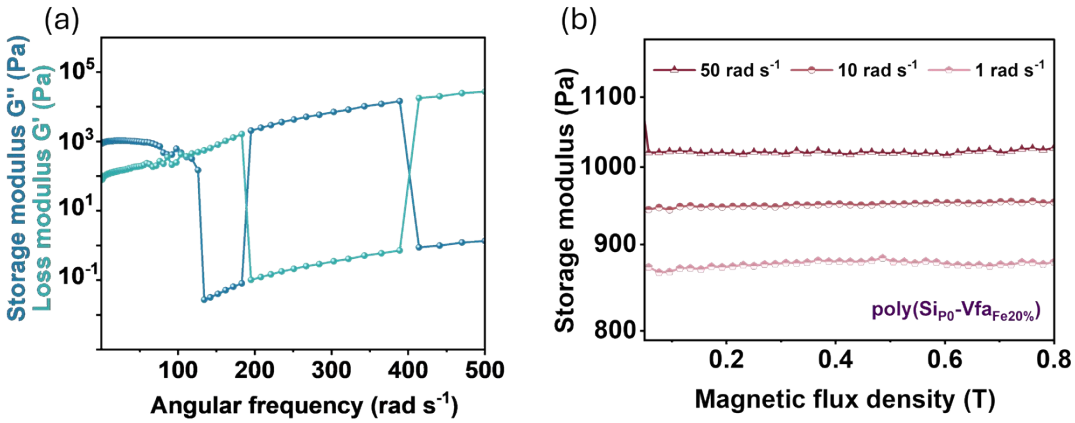

Figure S17. (a) Frequency sweep variation of the storage modulus (G″) and loss modulus (G′) of poly(Si_{P0}-Vfa) at constant magnetic flux (0.6 T), and (b) storage modulus of poly(Si_{P0}-$Vfa_{Fe20\%}$) with increasing magnetic field as a function of frequency.

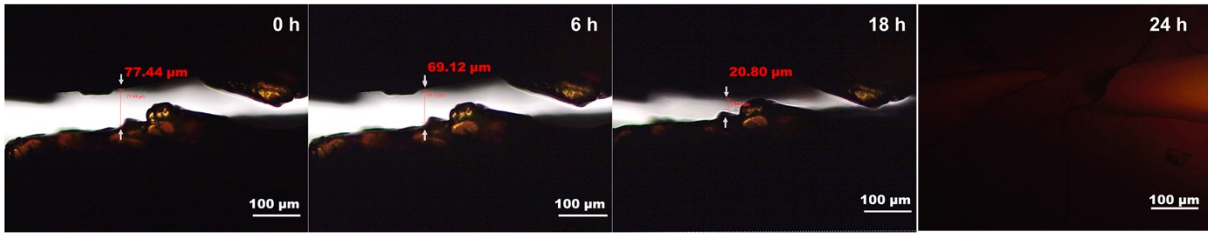

Figure S18. Time-dependent self-healing of scratch in poly(Si_{P0}-Vfa). Optical microscopic images of network at room temperature at different times.

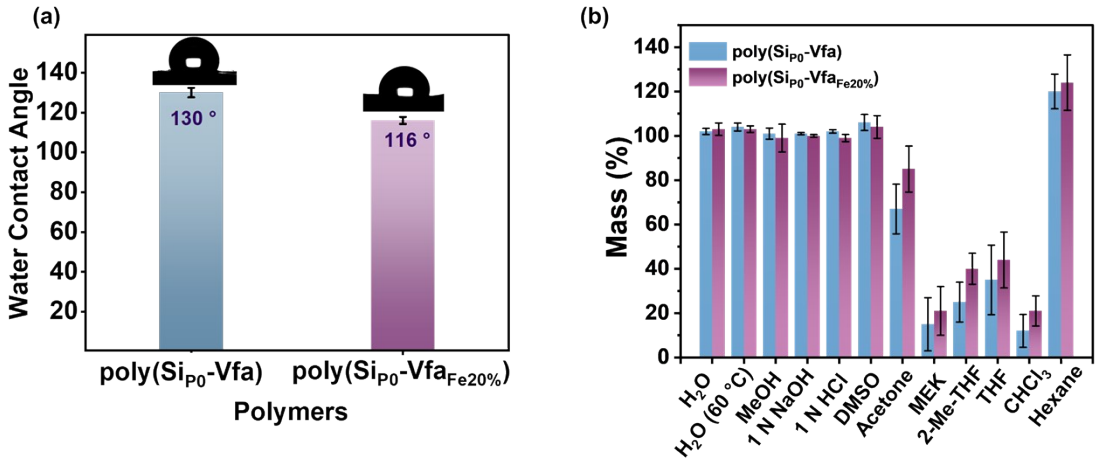

Figure S19. (a) Water contact angle (WCA) analysis of the polymers and (b) Variation of mass change of poly(Si_{P0}-Vfa) and poly(Si_{P0}-$Vfa_{Fe20\%}$) polymer networks in various solvents kept at 25 °C for 8 days.

Table S2. Summary of mass (%) change of poly(Si_{P0}-Vfa) and poly(Si_{P0}-$Vfa_{Fe20\%}$) polymer networks in various solvents at 25 °C for 8 days.

Solvent	**Polymers (% mass change)**	
	poly(Si_{P0}-Vfa)	poly(Si_{P0}-$Vfa_{Fe20\%}$)
H_2O	102 ± 0.5	103 ± 2.8
H_2O (60 °C)	104 ± 1.8	103 ± 1.5
MeOH	101 ± 2.5	99 ± 6.3
1 N NaOH	101 ± 0.5	100 ± 0.6
1 N HCl	102 ± 0.8	99 ± 1.6
DMSO	106 ± 3.6	104 ± 5.1
Acetone	67 ± 11.2	85 ± 10.4
MEK	15 ± 12.2	21± 11.0
2-MeTHF	25 ± 9	40 ± 7
THF	35 ± 15.7	44 ±12.6
$CHCl_3$	12 ± 18.5	21 ± 6.8
Hexane	120 ± 7.8	124 ± 12.5

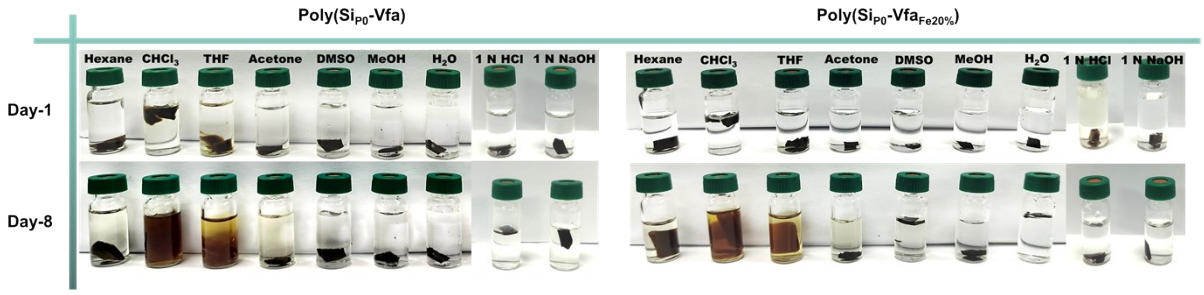

Figure S20. Digital images showing time-dependent solvent stability of vitrimers at room temperature.

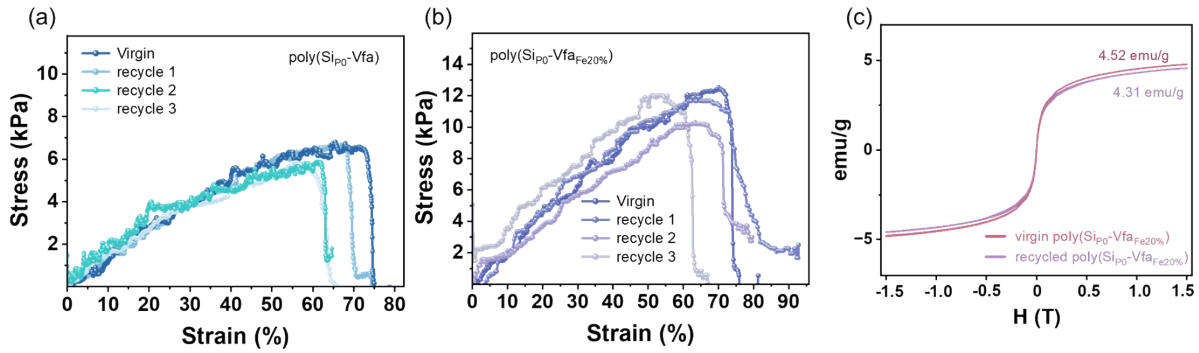

Figure S21. Tensile test curves of the recycled vitrimers over three consecutive cycles for (a) poly(Si$_{P0}$-Vfa) and (b) poly(Si$_{P0}$-Vfa$_{Fe20\%}$), along with (c) comparison of the magnetic hysteresis loops for the pristine and post-recycled magnetic vitrimer at 25 °C

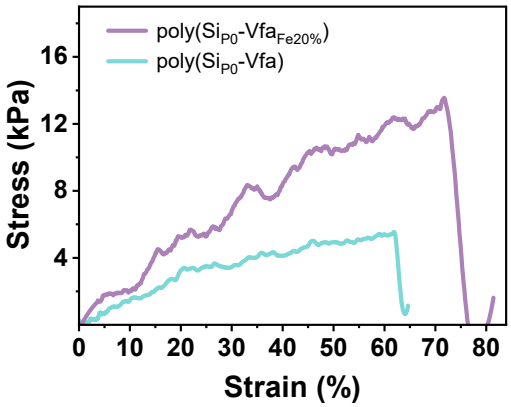

Figure S22. Tensile stress–strain curves of the vitrimers.

Table S3. Benchmark comparison of carbon-fibre-reinforced vitrimer composites and related soft vitrimer systems.

Materials	T_{max}‡ (°C)	E_a (kJ/mol)	Healing Temp (°C)	Functional Response	Mechanical Regime
Bio-epoxy elastomer (disulfide)[1]	300–350*	20–30	25	NR	Soft
PDMS–imine elastomer[2]	250–350*	N.D. 40–80*	25	NR	Soft
Siloxane–disulfide elastomer[3]	280–350*	N.D. 20–35*	25	NR	Soft
Multi-dynamic PDMS (disulfide + supramolecular)[4]	300–400*	20–40	25	NR	~1 MPa
CB/PDMS conductive elastomer[5]	300–400*	40–70	25	Electrical	Weak
Boronic vitrimer composite[6]	300–400*	60–100	~120	Magnetic	Moderate
Epoxy–siloxane vitrimer[7]	350–450*	80–150	~200	N.D.	Strong
PU vitrimer (imine)[8]	250–350*	~60	~90	N.D.	Moderate
PBZ vitrimer (imine)[9]	400–500*	80–120	~150	N.D.	Strong
PBZ dual dynamic exchange[10]	400–500*	50–90	~140	N.D.	Strong
PBZ–sulfur vitrimer[11]	350–450*	N.D. 30–80*	~120	N.D.	Moderate
PDMS-supramolecular elastomers[12]	250–350*	N.D. 20–40*	25	Electrical device	Soft
PU + Fe_3O_4@CNC[13]	250–300*	N.D.	25	Magnetic	Soft
MR plastomer (PCL/TPU)[14]	250–300*	N.D.	60	Magneto-rheological (MR)	Soft
PDMS + Fe_3O_4 composite[15]	300–400*	N.D.	25	Magnetic	Soft
PBZ + Fe_3O_4 composite[16]	400–500*	N.D.	N.D.	Magnetic (SMP)	Strong
Magnetoactive elastomer[17]	250–350*	N.D.	N.D.	MR	Soft
Magnetic ionic liquid[18]	>400	N.D.	N.D.	MR fluid	Liquid

Siloxane-BZ-Fe polymer[19]	350–500*	N.D.	50	Magnetic	Moderate
NIR-actuated PBZ[16]	400–500*	N.D.	~50	NIR actuation	Strong
Cardanol PBZ + Fe_3O_4 NPs[20]	350-400	N.D.	NA	Superparamagnetic	Strong

‡Determined from Thermogravimetry Analysis

*Thermal stability values were extracted from reported TGA curves or estimated based on polymer class when not explicitly provided.

†N.D. Not determined. Activation energies were taken from literature or given based on established ranges for corresponding dynamic chemistries.

N.R.: Not reported

References

1. S. Shan, D. Mai, Y. Lin and A. Zhang, *ACS Appl. Polym. Mater.*, **2021**, 3, 5115-5124.
2. P. Wang, L. Yang, B. Dai, Z. Yang, S. Guo, G. Gao, L. Xu, M. Sun, K. Yao and J. Zhu, *Eur. Polym. J.*, **2020**, 123, 109382.
3. L. Zhao, Y. Yin, B. Jiang, Z. Guo, C. Qu and Y. Huang, *J. Colloid Interface Sci.*, **2020**, 573, 105-114.
4. X. Shi, K. Zhang, L. Zhao, B. Jiang and Y. Huang, *Ind. Eng. Chem. Res.*, **2021**, 60, 2154-2162.
5. L. Bai, X. Yan, B. Feng and J. Zheng, *Compos. Part B Eng.*, **2021**, 223, 109123.
6. M. Cvek, J. Sevcik, J. Vilcakova, A. Athanassiou and A. Zych, *Appl. Mater. Today*, **2023**, 35, 101997.
7. T. Debsharma, V. Amfilochiou, A. A. Wróblewska, I. De Baere, W. Van Paepegem and F. E. Du Prez, *J. Am. Chem. Soc.*, **2022**, 144, 12280-12289.
8. P. Tan, X. Zhao, Z. Zhang, W. Wei, J. Zhou, Y. Shao, X. Ma, S. Wei, Z. Gao and S. Han, *ACS Appl. Polym. Mater.*, **2024**, 6, 8977-8988.
9. S. Zhang, J. Yi, J. Chen, Y. Li, B. Liu and Z. Lu, *ChemSusChem*, **2024**, 17.
10. Y. Li, Q. An, S. Chen, J. Zhang, H. Liu, S. Shao, L. Yin and Z. Wang, *Polymer*, **2025**, 339, 129173.
11. S. Sahu and B. Lochab, *ACS Sustainable Chem. Eng.*, **2024**, 12, 7126-7135.
12. H. Guo, Y. Han, W. Zhao, J. Yang and L. Zhang, *Nat. Comm.*, **2020**, 11.
13. Y. Wang, Q. Guo, G. Su, J. Cao, J. Liu and X. Zhang, *Adv. Funct. Mater.*, **2019**, 29, 1906198.
14. S. Qi, J. Fu, Y. Xie, Y. Li, R. Gan and M. Yu, *Compos. Sci. Technol.*, **2019**, 183, 107817.
15. H. Q. Tao, D. W. Yue and C. H. Li, *Macromol. Mater. Eng.*, **2022**, 307, 2100649.
16. S. Leungpuangkaew, L. Amornkitbamrung, N. Phetnoi, C. Sapcharoenkun, C. Jubsilp, S. Ekgasit and S. Rimdusit, *Adv. Ind. Eng. Polym. Res.*, **2023**, 6, 215-225.
17. D. Borin, G. Stepanov and E. Dohmen, *Arch. Appl. Mech.*, **2019**, 89, 105-117.
18. G. Sharma, S. Mitra, A. Bhattacharyya and S. K. Ghosh, *Soft Matter*, **2025**, 21, 4368-4377.
19. M. Arslan, B. Kiskan and Y. Yagci, *Macromolecules*, **2018**, 51, 10095-10103.
20. M. Monisha, N. Yadav, S. B. Srivastava, S. P. Singh and B. Lochab, *J. Mater. Chem. A*, **2018**, 6, 2555-2567.